

12-13-2001

Thermal effects in dynamics of interfaces

Alexander Umantsev

Fayetteville State University, aumantsev@uncfsu.edu

Recommended Citation

Umantsev, Alexander, "Thermal effects in dynamics of interfaces" (2001). *Natural Sciences Faculty Working Papers*. Paper 8.
http://digitalcommons.uncfsu.edu/natsci_wp/8

This Article is brought to you for free and open access by the College of Arts and Sciences at DigitalCommons@Fayetteville State University. It has been accepted for inclusion in Natural Sciences Faculty Working Papers by an authorized administrator of DigitalCommons@Fayetteville State University. For more information, please contact mLawson@uncfsu.edu.

Thermal effects in dynamics of interfaces

A. Umantsev

Department of Physics and Astronomy, Northern Arizona University, Flagstaff, Arizona 86011-6010

(Received 3 October 2001; accepted 13 December 2001)

Dynamical Ginzburg–Landau theory is applied to the study of thermal effects of motion of interfaces that appear after different phase transitions. These effects stem from the existence of the surface thermodynamic properties and temperature gradients in the interfacial transition region. Thermal effects may be explained by the introduction of a new thermodynamic force exerted on the interface, called here Gibbs–Duhem force, and the internal energy density flux through the interface. The evolution equations for the interfacial motion are derived. For the experimental verification of the thermal effects during continuous ordering the expression is derived for the amplitude of temperature waves. © 2002 American Institute of Physics. [DOI: 10.1063/1.1448485]

I. INTRODUCTION

An interface comprises a layer of rapid variations of structural properties and is an important paradigm in science that helps understand many, seemingly unrelated, physical situations. Commonly interfaces appear whenever a thermodynamic system undergoes some kind of a phase transition and may be encountered in condensed matter, soft matter (biology) and even cosmology. Interfaces constitute structural defects and, because of the global disequilibrium of a defective system, a network of interfaces exhibits structural coarsening or time evolution of the interface density. Three distinctly different types of interfaces may be identified in different thermodynamic systems: (1) homophase interfaces, which separate two bulk pieces of the same phase and same composition, e.g., grain boundaries, Bloch (magnetic) walls, antiphase-domain boundaries, and Higgs field boundaries in cosmology; (2) isomorphous interfaces between phases of the same crystalline structure but significantly different composition, e.g., polymeric interfaces, which occur commonly via spinodal decomposition; (3) heterophase interfaces, which appear as a result of different first-order (discontinuous) phase transitions, e.g., crystallization, and separate phases of different crystalline symmetry. In the present paper, however, we will not be concerned with specific model systems or types of transitions. Rather, we will be concerned with the general features of interfacial dynamics and thermal effects that may manifest in completely unrelated situations. For instance, for the first time heterophase and homophase interfaces are treated on the common basis.

Moving interfaces are exposed to different thermal effects that were studied mainly for first-order transitions, like melting–freezing, where emission or absorption of the latent heat associated with the transition renders a “feedback” reaction on the rate and microstructure of the transformation. In order to study thermal effects, naturally, we need a heat equation compatible with the dynamics of phase transitions that take place in the system. There is a whole bunch of different models now “on the market” that describe such situation. The history of application of the heat equation to thermodynamic systems with relaxation goes back to the

early 1950s in the Russian literature when Fastov¹ used “the entropy version” to study relaxations in elastic media (no phase transitions). Later Patashinski *et al.*^{2,3} and Oxtoby *et al.*⁴ independently applied such an equation to the problem of phase boundary motion. Halperin, Hohenberg, Ma⁵ were the first to propose on semi-intuitive grounds an ad hoc “energy version” of the heat equation which they dubbed Model C. In mid-1980s Caginalp, and Collins and Levine⁶ introduced the “phase-field” model, which includes the heat equation with constant density of heat sources equal to the latent heat of transformation. The phase-field model serves the purpose of being an effective numerical tool, at the same time yielding a reasonable approximation in the limiting case of a sharp interface.⁷ Although intuitively appealing, the phase field model is not thermodynamically consistent with the dynamics of phase transitions, which precludes it from revealing all physical effects that accompany the transitions.

The topic of thermodynamic consistency of the heat equation with the phase transitions was recently a subject of extensive scrutiny and several attempts^{8,9} have been made to derive one. These attempts, however, suffer from one major problem that not all energy contributions were accounted for in the internal energy functional of the whole system. That did not allow the authors to derive the full expression for the heat source and capture all essential thermal effects in the system. As known, the heat equation may be derived from the first or second law of thermodynamics utilizing the energy or entropy function and must lead to the same equation.¹⁰ A thermodynamically consistent derivation of the generalized heat equation compatible with the first and second laws and dynamics of phase transitions was first presented in Ref. 11 and will be briefly reviewed in Sec. III A. Such equations can be used not only for phase transitions but also for any thermodynamic process where internal parameters relax in the course of the latter.

Thermal effects may alter the course not only of first-order transitions but of the continuous transitions as well, especially in systems with low thermal conductivity. Zia *et al.*¹² considered the dynamics of the interface between two

symmetric phases using the framework of the so-called Model C.⁵ Although being a right step in the right direction, this work lacks any quantitative results on the part of interface kinetics except the morphological stability. Recently we analyzed the influence of the internal energy excess on the dynamics of the antiphase domain boundary in the framework of the Onsager theory of linear response.¹³ We derived an evolution equation that takes into account the finite rate of energy transfer in the transition region and showed that the internal energy transport causes a drag effect and temperature hump in the transition region. Although the principal result that the necessity to move energy together with the interface results in slowing down of its motion was obtained in the paper on the grounds of simple symmetry arguments, some questions remained unanswered. For instance, what is the temperature distribution around the interface? What will happen if the energy transfer mechanism (thermal conduction) is turned off?

To answer these questions, motion of a homophase boundary will be analyzed here in the framework of the dynamical Ginzburg–Landau theory, which, arguably, is the most convenient way of addressing such problem. The paradigm of the Landau theory of phase transition¹⁵ assumes that the Gibbs free energy in addition to temperature and pressure is a continuous function of the long-range order parameters with different transitions corresponding to different order parameters. In this paper we shall restrict ourselves with systems that exhibit nonconservative dynamics of the order parameter only. To wit, the conservative dynamics of spinodal decomposition in solutions of small molecules and polymer blends are not included in the consideration here. Thermal effects in the latter were considered in Ref. 14. All other cases of interfaces presented above will be treated here on the common grounds of the dynamical Ginzburg–Landau theory.

The scope of the paper is as follows: In Sec. II the isothermal dynamics of interfaces in systems without any conservative law will be reviewed. In Sec. III thermal effects of interfacial dynamics are considered and a local evolution equations are derived. In Secs. IV and V these equations are applied to two different types of interfaces, homophase and heterophase. In Sec. VI the main results are discussed and an experiment to reveal thermal effects in new systems is suggested.

II. ISOTHERMAL DYNAMICS OF INTERFACES

A. Landau theory of phase transitions

Any theory of dynamic processes starts with the analysis of the equilibrium state in the system, specified by the conditions on its boundary, e.g., constant temperature and pressure (open system), or adiabatic insulation from the environment (closed system). One has to choose the set of independent variables and conjugate dependent thermodynamic functions that characterize such state of equilibrium. Away from equilibrium, in addition to temperature T and pressure P , a thermodynamic system is characterized by another set of internal parameters $\{\eta_i\}$, which is a measure of disequilibrium in the system. Then, criteria of equilibria in

different systems are expressed as the conditions of optimization of specified thermodynamic functions, e.g., Gibbs free energy G , internal energy E , or entropy S with respect to variations of this set of internal parameters $\{\eta_i\}$,

$$\Phi = \left(\frac{\delta E}{\delta \eta_i} \right)_{S,V} = \left(\frac{\delta G}{\delta \eta_i} \right)_{T,P} = -T \left(\frac{\delta S}{\delta \eta_i} \right)_{E,V} = 0. \quad (1)$$

One may argue that temperature and pressure is a better choice of independent variables than energy density and specific volume because, regardless of the outer constraints of open or closed systems, conditions of equilibrium, together with Eq. (1), include constant temperature and pressure throughout, but not constant energy density or specific volume. These arguments determine our choice of (T,P) as the independent variables and the Gibbs free energy G as the thermodynamic potential. At equilibrium the internal parameters relax to specific values which are functions of temperature and pressure, $\eta_i^E = \Xi(T,P)$, and can be found by resolving the proper condition of thermal equilibrium (1). Entropy S , volume V , and other thermodynamic functions may be found with the help of the Legendre transformation,

$$S = - \left(\frac{\partial G(T,P, \eta_i)}{\partial T} \right)_{P, \eta_i}, \quad V = \left(\frac{\partial G(T,P, \eta_i)}{\partial P} \right)_{T, \eta_i},$$

$$G(T,P, \eta_i) = E - TS + PV. \quad (2)$$

In the framework of the Landau theory of phase transitions¹⁵ the internal parameters $\{\eta_i\}$ are associated with the symmetry changes and are usually called the order parameters (OP). The concept of an order parameter helps define a *phase* as a locally stable state of matter homogeneous in the order parameter. Different transitions may be laid out into the same framework if proper physical interpretations of order parameters are found. All examples from the Introduction may be described by a single scalar order parameter: magnetization for ferromagnets, average angle of molecules about the direction of the director for liquid crystals, ordering on sublattices for order–disorder transition, scalar Higgs field in cosmology. That is why we restrict the present paper to the case of a scalar OP η .

In the framework of a Landau theory¹⁵ the free energy is a continuous function of OP and may be expanded in powers of OP compatible with the symmetries of initial and final phases,

$$G(T,P, \eta) = G(T,P,0) + V \left\{ \frac{1}{2} a(T,P) \eta^2 + \frac{1}{3} b(T,P) \eta^3 + \frac{1}{4} c(T,P) \eta^4 + \dots \right\}. \quad (3)$$

Commonly, the temperature dependent coefficients of the expansion $a(T)$, $b(T)$, $c(T)$, ... are taken in the Landau form where the first one is linearly proportional to temperature, $a(T) = a_0(T - T_c)$, and b , c are temperature independent.

B. Interfaces at equilibrium

Coexistence of two phases at equilibrium brings about a transition region between them, called an *interface*. The presence of interfaces makes the system essentially inhomogeneous even at equilibrium that is, there appear gradients of

OP. Since an interface comprises the spatial variation of the OP, the Gibbs free energy of the entire system should be written in the functional form,

$$G = \int \hat{g} d^3x. \quad (4)$$

The free energy density \hat{g} becomes a function of the gradients of the thermodynamic variables as well as the variables themselves. There is a certain penalty on the inhomogeneous system in the form of the “gradient energy” contribution into the free energy. In this paper the gradient-energy contribution is represented in the standard Ginzburg–Landau–Cahn–Hilliard form,^{16,17}

$$\hat{g} = g(T, P, \eta) + \frac{1}{2} \kappa (\nabla \eta)^2, \quad (5)$$

where the gradient energy coefficient κ may depend on temperature and pressure.

Thermodynamic equilibrium of the system under conditions of constant temperature and pressure is described by minimization of the Gibbs free energy, Eq. (1). For the functional (4), (5), the latter takes the form of the Euler–Lagrange equation,

$$\frac{\delta G}{\delta \eta} \equiv \frac{\partial g}{\partial \eta} - \kappa \nabla^2 \eta = 0. \quad (6)$$

At constant temperature and pressure. Eq. (6) is known to have many different solutions with different symmetries, e.g., one-dimensional periodic,¹⁸ cylindrical, spherical.¹⁹ None of these, however, possess thermodynamic stability except one-dimensional translation invariant solutions, which represent flat interfaces. Using translation invariance, Eq. (6) may be integrated once to yield

$$\check{g}(T_E, P_E, \eta) \equiv g(T_E, P_E, \eta) - \frac{\kappa}{2} \left(\frac{d\eta}{dx} \right)^2 = \mu, \quad (7)$$

where (T_E, P_E) are the equilibrium temperature and pressure, that is the temperature and pressure of phase coexistence, and μ is the chemical potential, which may be found from the values of the free energy far away from the interface,

$$\mu = g(T_E, P_E, \eta_+) = g(T_E, P_E, \eta_-). \quad (8)$$

Equation (8) is a continuum expression of the Gibbs phase rule. Here and below $\varphi_{\pm} \equiv \varphi(x = \pm\infty)$ and $\eta_{\pm} = \Xi(T_E, P_E)$ are the equilibrium bulk-phase OP values. In Eqs. (5), (7) and below the hatted quantities stand for non-local densities and are defined as the sum of the local and gradient contributions, while the quantities with \cup are defined as the differences of the same contributions. An analogy with the classical mechanics may be brought to bear: \check{g} is analogous to the negative of the Hamiltonian of the mechanical system, the nonlocal free energy density—to the Lagrangian, and the total free energy—to the action. Then Eq. (6) is equivalent to the Lagrange equation, Eq. (7)—to the conservation of the mechanical energy with μ being the total energy.

For the free energy (3) to describe a phase transition it ought to have a characteristic double-well form. Then Eq. (7) may be solved to yield a typical hyperbolic tangent shape for

the OP variation through the interface, $\eta_l(x)$. Different types of interfaces with respect to their stability at different temperatures are considered in the Secs. IV and V.

As is known,^{20,21} all properties of an interface at equilibrium are completely determined by just one intensive quantity, the surface tension or *surface energy* σ . The equilibrium surface energy in a one-component medium is defined as the excess Gibbs free energy of the system with an interface, per unit area of the interface, compared to that of the homogeneous bulk phase occupying the same volume. The corresponding extensive quantity is proportional to the total area of the interface. Utilizing Eqs. (4), (8) for σ , we obtain^{17,22}

$$\sigma \equiv \int_{-\infty}^{+\infty} \{ \hat{g}(T_E, P_E, \eta_l) - \mu \} dx. \quad (9)$$

Equations (5), (7), (9) yield another expression for the surface energy,

$$\sigma = \int_{-\infty}^{+\infty} \kappa \left(\frac{d\eta_l}{du} \right)^2 du. \quad (10)$$

To characterize an interfacial thickness we adopt the definition introduced in Ref. 17,

$$l_l \equiv \frac{[\eta_l]}{\max |\nabla \eta_l|}, \quad (11)$$

where a quantity in square brackets represents the jump across the interface: $[\varphi] \equiv \varphi_+ - \varphi_-$. Then Eqs. (5), (7), (10), (11) allow us to estimate the surface tension as $\sigma \approx \kappa [\eta_l]^2 / l_l$. It is also advantageous for our analysis to introduce the following surface quantity,²²

$$\Gamma_s \equiv \int_{-\infty}^{+\infty} \delta s dx, \quad (12)$$

$$\delta s = \left\{ \hat{s} - s_+ - (\eta - \eta_+) \frac{[s]}{[\eta]} \right\}. \quad (13)$$

The quantity Γ_s does not diverge and, in the spirit of Gibbs,²⁰ may be called the relative surface entropy with respect to the OP.

C. Relaxation of an order parameter

Being away from equilibrium the thermodynamic system relaxes back to an equilibrium state where the OP is one of the solutions of Eq. (1). Hence, Φ is the driving force for the OP relaxation. Mandel'shtam and Leontovitch implemented this idea in a seminal paper²³ where they studied relaxations and scattering of sound in liquids (no phase transitions).²⁴ To characterize relaxation in a nonequilibrium system in compliance with the second law they assumed linear proportion between the rate of the relaxation parameter change and the thermodynamic force Φ : $\dot{\eta} \propto -(\partial G / \partial \eta)_{T,P}$. Landau and Khalatnikov adopted this evolution equation later in their study of the absorption of sound in the vicinity of the second-order transition.²⁵

In heterogeneous medium the gradient-energy contribution is essential and the free energy is a functional (4), (5). Therefore, the local thermodynamic force is expressed as the

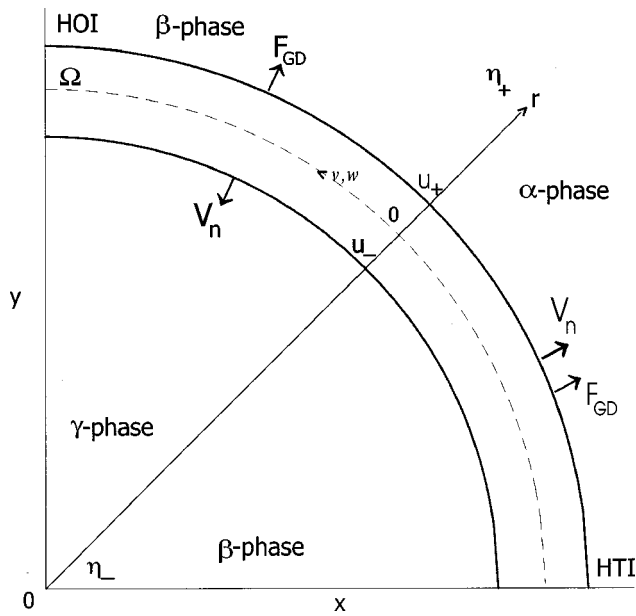


FIG. 1. Curvilinear coordinate system (u, v, w) associated with a moving interface. The Gibbs–Duhem force F_{GD} may be either parallel or antiparallel to the interfacial velocity V_n depending on the type of interface heterogeneous (HTI) or homogeneous (HOI).

variational derivative of the free energy [left-hand side of Eq. (6)] instead of the partial one and the general equation of the order parameter evolution takes the form, which is known as the time-dependent Ginzburg–Landau equation (TDGLE),

$$\frac{d\eta}{dt} = -\gamma \left(\frac{\delta G}{\delta \eta} \right)_{T,P}. \quad (14)$$

Here d/dt means the substantial derivative. The response coefficient γ sets the relaxation time scale $\tau_\eta = (\gamma a)^{-1}$.

D. Interfaces away from equilibrium

Consider a transition from one state to another when the OP changes its bulk-phase value from η_+ to η_- very rapidly inside a certain transition zone, called interface, while remaining practically constant or changing very slowly outside this zone, see Fig. 1. To describe motion of a curved interface away from equilibrium, instead of the Cartesian coordinate system $\mathbf{x} = (x, y, z)$, we shall introduce new *curvilinear time-dependent coordinates* $\{u = U(\mathbf{x}, t), v = V(\mathbf{x}, t), w = W(\mathbf{x}, t)\}$ such that the OP is a function of one coordinate only: $\eta = \eta(u)$.^{11,26–30} One may introduce the velocity of motion $V_n(v, w, t)$ of the surface $U = \text{const}$ using the relation,

$$\frac{\partial U}{\partial t} + V_n |\nabla U| = 0. \quad (15)$$

In order to eliminate the arbitrariness of the new curvilinear coordinates associated with the transformation function $u = U(\mathbf{x}, t)$, we assume that it obeys the eikonal equation everywhere: $(\nabla U)^2 = 1$.^{31,32} Hence, the $U = \text{const}$ surfaces are equidistant and the radius of curvature of these surfaces is $r = r_0(v, w, t) + u$, where $r_0(v, w, t)$ is the radius of curvature of the surface $U = 0$, see Fig. 1. The latter is specified as

follows: $d^2 \eta(0)/du^2 = 0$. According to Eqs. (1), (6), $\eta(0)$ corresponds to one of the equilibrium values of the OP: $\eta^E = \Xi(T, P)$.

The Laplacian operator can be conveniently expressed in the new coordinates as follows:

$$\nabla^2 = \frac{\partial^2}{\partial u^2} + 2K(u, v, w, t) \frac{\partial}{\partial u}, \quad (16)$$

where K is the mean curvature of the surface $U = \text{const}$,^{33,34}

$$K \equiv r^{-1}(u, v, w, t) = K_0 \{1 - uK_0 + u^2 K_0^2 + O(u^3 K_0^3)\}; \quad (17)$$

$$K_0 = K(0, v, w, t).$$

In the curvilinear coordinates TDGLE (14) transforms into an ODE as follows:^{11,26–30}

$$\kappa \frac{d^2 \eta}{du^2} + \left(2\kappa K + \frac{V_n}{\gamma} \right) \frac{d\eta}{du} - \frac{\partial g(T, \eta)}{\partial \eta} = 0. \quad (18)$$

Introduction of the time-dependent curvilinear coordinates has an advantage in that the evolution of the OP field may be described now by the motion of one surface $U = 0$ in space and time. This method is reminiscent of the method of characteristics in hydrodynamics and theory of sound¹⁰ and the method of the optical path in the theory of light.^{31,32} To solve Eq. (18) the method of averaging will be used in the next section.

It is also possible, however much less trivial than at equilibrium, to determine the surface energy of an interface, which is allowed to move. The major difficulty comes from the fact that the free energy densities of phases on opposite sides of the interface are not supposed to be equal in disequilibrium. On the contrary, if present (e.g., for a first-order transition), the difference between these densities constitutes the bulk driving force for the interface motion. Even if the densities of the free energy are equal (e.g., for a continuous transition), the interface is not flat and is moving under influence of its own curvature and surface energy. To find the nonequilibrium surface energy we suggest the following procedure.³⁵ Let us allow the interface to move during dt and calculate the change of the Gibbs free energy in the system as a result of such motion, assuming temperature a constant. Using Eqs. (4), (6), we obtain

$$dG = \int (\delta \hat{g})_T d^3x = dt \int \left[\left(\frac{\partial g}{\partial \eta} \right)_T - \kappa \nabla^2 \eta \right] \frac{d\eta}{dt} d^3x. \quad (19)$$

Transforming to the curvilinear coordinates (u, v, w) and using Eqs. (15), (16), (17), one can find that this change is divided into two contributions,

$$dG = -dt \cdot [g] \cdot \int_{\Omega} V_n dv dw + dt \cdot \int_{u_-}^{u_+} \kappa \left(\frac{d\eta}{du} \right)^2 du \cdot \int_{\Omega} 2K_0 V_n dv dw. \quad (20)$$

Here u_- and u_+ are the points far from the interface where $d\eta/du$ vanishes and Ω is the area of the interface, Fig. 1. The first term is proportional to the volume of the material swept over by the interface; the coefficient of proportionality in front of this term is the bulk free-energy jump that represents

the driving force for the interface motion. The second term is proportional to the change of the area of the interface; the coefficient of proportionality of this term is the nonequilibrium surface energy.

The fact that the formula for the nonequilibrium surface energy coincides with that at equilibrium Eq. (10), allows us to introduce the surface entropy χ and internal energy ε as follows:

$$\chi \equiv -\frac{d\sigma}{dT}; \quad \varepsilon \equiv \sigma + T\chi. \quad (21)$$

If an equilibrium interface exists at a specific temperature T_E only, as is the case for a first-order transition, the differentiation in Eq. (21) should be understood in the sense of disequilibrium. Otherwise, for instance in case of a continuous transition, the surface entropy χ equals the relative surface entropy Γ_s , Eq. (12). The equilibrium definition of the interfacial thickness, Eq. (11), may also be extended into a nonequilibrium situation of a moving boundary. As one can see from Eqs. (16), (17), (19), (20), the separation of the free energy change into volumetric and interfacial contributions is possible only if the geometric number of the interface is small enough,

$$Ge \equiv 2K_0 l_I \ll 1. \quad (22)$$

III. THERMAL EFFECTS OF INTERFACIAL DYNAMICS

A. Generalized equation of heat transfer

As it has been concluded in the Introduction, the motion of an interface is accompanied by energy redistribution and heat propagation in the system. In order to derive the generalized heat equation (GHE), which describes temperature variations along with ongoing phase transition, one has to apply the first law of thermodynamics to a small volume δV of a heterogeneous nonequilibrium medium, $d\hat{e} = \delta q + \delta w$. Here δw is the work term and $\delta q = -\text{div } J_T dt$ is the amount of heat given to the volume δV . As the compression is not the issue in this paper, we will assume our medium incompressible. Hence, the work term vanishes. To finish the GHE one has to find the expressions for the internal energy density variation $d\hat{e}$ and the heat flux \mathbf{J}_T that account for nonlocal interactions in the medium.

The derivation of the former¹¹ is based on the calculation of a small variation of the internal energy functional E of the whole system as a result of a small *inhomogeneous* variation of the OP $\delta\eta$,

$$\delta E = \int_{\delta V} (\delta\hat{e}) d^3x. \quad (23)$$

Now let us assume that the variation $\delta\eta$ occurred in the volume δV *independently* from neighboring volumes of the system and at constant temperature. Such variation $\delta\eta$ vanishes everywhere outside of the considered volume. Then, using the definition of the variational derivative,³⁶ we obtain

$$\delta E = \frac{\delta E}{\delta\eta} \int_{\delta V} (\delta\eta) d^3x. \quad (24)$$

Finally, comparing Eqs. (23) and (24) and using continuity of the variations $\delta\hat{e}(\mathbf{x})$ and $\delta\eta(\mathbf{x})$ as functions of the position, we arrive at the expression for the energy density variation,

$$\delta\hat{e} = \left(\frac{\delta E}{\delta\eta} \right)_{V,T} \delta\eta. \quad (25)$$

When temperature varies simultaneously with OP the nonlocal energy density variation takes the form,

$$d\hat{e} = C dT + \left(\frac{\delta E}{\delta\eta} \right)_{V,T} d\eta; \quad C \equiv \left(\frac{\partial \hat{e}}{\partial T} \right)_{V,\eta}. \quad (26)$$

Here C is the specific heat for constant V and η per unit volume of such material.

Substitution of Eq. (26) into the first law of thermodynamics for the incompressible medium yields the GHE sought for

$$C \frac{dT}{dt} = -\nabla \mathbf{J}_T + Q(\mathbf{x}, t), \quad (27)$$

where $Q(\mathbf{x}, t)$ is the density of instantaneous heat sources in the energy representation,

$$Q(\mathbf{x}, t) = - \left(\frac{\delta E}{\delta\eta} \right)_{V,T} \frac{d\eta}{dt} = - \left[\left(\frac{\partial e}{\partial \eta} \right)_{V,T} - \kappa_E \nabla^2 \eta \right] \frac{d\eta}{dt}, \quad (28)$$

$$\kappa_E = \kappa - T \frac{d\kappa}{dT}.$$

Utilizing Legendre transformation, Eqs. (2), the heat source $Q(\mathbf{x}, t)$ may also be represented in the entropy form,

$$Q(\mathbf{x}, t) = - \left[T \left(\frac{\delta S}{\delta\eta} \right)_{V,T} + \left(\frac{\delta G}{\delta\eta} \right)_{V,T} \right] \frac{d\eta}{dt}. \quad (29)$$

The same variational procedure as in Eqs. (23)–(26) may be used to find the entropy variation in the volume δV ,

$$d\hat{s} = \frac{C}{T} dT + \left(\frac{\delta S}{\delta\eta} \right)_{V,T} d\eta; \quad C = T \left(\frac{\partial \hat{s}}{\partial T} \right)_{V,\eta}. \quad (30)$$

Comparing Eqs. (30) and (26) and using Eq. (29) we arrive at the expression of the first law in the form,

$$d\hat{s} = \frac{1}{T} \delta q - \frac{1}{T} \left(\frac{\delta G}{\delta\eta} \right)_{V,T} d\eta. \quad (31)$$

According to the second law of thermodynamics $d\hat{s} \geq \delta q/T$. Application of the second law to our system yields a constraint on the OP evolution equation,

$$\left(\frac{\delta G}{\delta\eta} \right)_{V,T} \frac{d\eta}{dt} \leq 0. \quad (32)$$

Constraint (32) was first derived in Ref. 11 and rederived later in Ref. 9. It manifests the Le Chatelier–Braun principle in the nonlocal nonequilibrium media and proves that the TDGLE (14) is admissible, but not a unique, choice of the evolution equation for the OP if the response coefficient γ is positive. Another option for the OP would be to obey

an evolution equation with memory,³⁷ $\dot{\eta} = -\int^t A(t-s)\Phi(s)ds$. In this case, condition (32) yields positive definiteness of the kernel $A(t)$.

The entropy representation, Eq. (29), shows that the heat source consists of the entropy contribution, which may be either positive or negative depending on the direction of the transition, and the dissipation which, due to the constraint (32), is proportional to the rate of the transition squared and, hence, always positive. Also it is possible to see from the entropy representation, Eq. (29), that there may be local sinks of heat inside an overall positive heat source.

The heat flux in a thermodynamic system \mathbf{J}_T depends on local values of temperature, its gradients and properties of the medium. In Refs. 5 and 9 the following expression was adopted for the flux: $\Lambda \nabla(\delta S/\delta \hat{\epsilon})$. Another possibility would be to consider an integral expression for the heat flux in a medium with memory.³⁸ The heat flux vector, however, is known to vanish with ∇T (Fourier's Law). Thus expanding the flux \mathbf{J}_T in ∇T and disregarding terms of the order higher than the first one we obtain the regular expression for the heat flux, $\mathbf{J}_T = -\lambda \nabla T$, where the thermal conductivity λ may be a function of T and η . Then the GHE takes the form,

$$C \frac{dT}{dt} = \nabla(\lambda \nabla T) + Q(\mathbf{x}, t). \quad (33)$$

GHE, Eqs. (28), (29), (33), is thermodynamically rigorous and absolutely invariant with respect to the derivation from the first or second laws of thermodynamics. The system of coupling TDGLE (14) and GHE (33) describes creation and subsequent evolution of an interface in a medium. Both equations, are of diffusion type and are characterized by diffusivities, the thermal diffusivity $\alpha = \lambda/C$ for the latter and the ordering diffusivity $m = \gamma\kappa$ for the former. The ratio of these diffusivities R is an important parameter, which determines different regimes of interfacial dynamics,

$$R \equiv \frac{\alpha}{m}. \quad (34)$$

As it has been explained in the Introduction, a few other forms of the GHE have been suggested and derived. No one of them, however, is complete in the sense of all relaxation effects being accounted for. The "entropic version" of the GHE, suggested and used in Refs. 1-4, lacks the dissipative term proportional to the rate squared, second term in the entropic representation of the heat source, Eq. (29). The "energetic version" of GHE, suggested and used in Refs. 5, 8, 9, lacks the nonlocal nonequilibrium term, the last term in the energetic representation of the heat source, Eq. (28). The latter stems from the fact that the gradient energy was not accounted for in the total internal energy functional that is, the nonlocal interactions in the system were assumed to be completely of entropic nature. It will be shown in the next section that this term is solely responsible for the surface creation and dissipation effect in the motion of interfaces.

B. Energy density flux

A phase transition is accompanied by the transfer of the internal energy, which is described by the energy density flux

vector \mathbf{J}_E , defined as follows: $d\hat{\epsilon}/dt = -\text{div} \mathbf{J}_E$. As we are concerned with transition in incompressible media, $d/dt = \partial/\partial t$ and, in order to obtain an expression for the energy density flux, we should find the partial derivative of $\hat{\epsilon}$ with respect to time,

$$\frac{\partial \hat{\epsilon}}{\partial t} = C \frac{\partial T}{\partial t} + \frac{\delta E}{\delta \eta} \frac{\partial \eta}{\partial t} + \text{div} \left(\kappa_E \nabla \eta \frac{\partial \eta}{\partial t} \right). \quad (35)$$

Substituting the GHE in the energetic representation, Eqs. (27), (28), into Eq. (35) we obtain the expression for \mathbf{J}_E in the incompressible motionless medium,

$$\mathbf{J}_E = \mathbf{J}_T - \kappa_E \nabla \eta \frac{\partial \eta}{\partial t}. \quad (36)$$

This is a new result. It shows that except for the heat flux, the expression for \mathbf{J}_E contains the work flux associated with the interactions that appear in the system due to inhomogenities in a nonlocal nonequilibrium medium. The work flux entails the inhomogeneous term in the heat source, Eq. (28), and is responsible for the surface creation and dissipation effect, analyzed in the next section. The work flux is analogous to the intensity of a sound wave in a fluid with η replacing the displacement of an element of fluid and κ_E replacing the adiabatic bulk modulus.¹⁰

C. Evolution equation for nonisothermal interfaces

In order to derive the evolution equation for a piece of an interface we transform TDGLE (14) and GHE (33) to the time-dependent curvilinear coordinates (u, v, w) , where $\eta = \eta(u)$ and $T = T(u, v, w)$. In the new curvilinear coordinates TDGLE is represented by Eq. (18) and GHE, Eq. (33), transforms as follows:

$$C \frac{\partial T}{\partial t} = \lambda \frac{\partial^2 T}{\partial u^2} + (2\lambda K + CV_n) \frac{\partial T}{\partial u} + Q \left(T, \eta, \frac{d\eta}{du} \right). \quad (37)$$

Then we average these equations over the thickness of the interface. Proper averaging of the TDGLE should include a weight factor because at equilibrium $-\int^+ \partial g / \partial \eta (T_E, \eta_I) du = 0$, see Eq. (7). Contrary to that, we do not need any weight factors to average GHE (37) because $-\int^+ Q(T_E, \eta_I) du \neq 0$. We multiply all the terms of Eq. (18) by the weight factor $d\eta/du$ and integrate them over the interval (u_-, u_+) . Utilizing the relation,

$$dg = \frac{\partial g}{\partial \eta} d\eta + \frac{\partial g}{\partial T} dT, \quad (38)$$

and taking into account that $d\eta/du$ vanishes at u_- and u_+ we obtain an equation for the motion of a phase separating interface,

$$\int_{u_-}^{u_+} \left(2\kappa K + \frac{V_n}{\gamma} \right) \left(\frac{d\eta}{du} \right)^2 du = [g] + \int_{u_-}^{u_+} \check{s} \frac{\partial T}{\partial u} du, \quad (39)$$

where $\check{s} = s - 1/2\kappa_s(d\eta/du)^2$ and $\kappa_s = -d\kappa/dT$. Using Eq. (17) and the fact that $(d\eta/du)^2$ is a bell-like, even function of u , the left-hand side of Eq. (39) may be represented as follows:

$$\sigma k_\eta + O(l_I^3 K_0^3), \quad (40)$$

where σ is the nonequilibrium surface energy, see Eqs. (10), (20), and k_η may be called the dynamic wave number of a curved interface,

$$k_\eta = \frac{V_n}{m} + 2K_0. \quad (41)$$

The first term in the right-hand side of Eq. (39) is the free energy jump across the interface where temperature changes together with OP. The physical nature of this term may be elucidated by the introduction of the latent heat of a transition at temperature T ,^{40,41}

$$L(T) \equiv [e]_T. \quad (42a)$$

Such definition yields the relation for the specific heat jump across the interface, cf. Eq. (26),

$$\frac{dL}{dT} = [C]_T. \quad (42b)$$

Notice that the jump of e and C in Eqs. (42) must be taken at constant temperature and the differentiation in Eq. (42b) is *not* along the equilibrium curve, as in Ref. 40. Then, the free energy jump in a system where the latent heat is temperature independent can be expressed as follows:

$$[g] = L \frac{T_E - T_-}{T_E} - s_+[T] + C \left\{ [T] - T_- \ln \left(1 + \frac{[T]}{T_-} \right) \right\}. \quad (43)$$

Substituting Eqs. (40) and (43) into Eq. (39) we obtain an evolution equation which relates different local characteristics of an interface,

$$\sigma k_\eta = L \frac{T_E - T_-}{T_E} + F_{GD} + \frac{1}{2} C \frac{[T]^2}{T_-} + O([T]^3, l_I^3 K_0^3), \quad (44a)$$

$$F_{GD} \equiv \int_{u_-}^{u_+} (\check{s} - s_+) \frac{\partial T}{\partial u} du. \quad (44b)$$

Equation (44) reveals the ‘‘driving forces’’ for the interfacial motion and is the principal result of the present paper. According to Eq. (44a), an interface is driven not only by its curvature ($-2K_0$) and the free energy difference on both sides of the interface, $L(T_E - T_-)/T_E$, but also by another force, F_{GD} , which appears as a consequence of the temperature gradient inside the transition zone, see Eq. (44b). Such force may be called the *Gibbs–Duhem force* because it may be found from the Gibbs–Duhem relation. Notice that the driving forces in Eq. (44a) have units of pressure because they act on a unit area of the interface.

To elucidate the physical meaning of F_{GD} we solve the stationary GHE (37) ($\partial T/\partial t = 0$) inside the interface using a method of asymptotic expansion. First, we obtain integral

representations of the temperature gradient when the temperature gradient in the final phase at $u = u_-$ is zero and we integrate this expression by parts,

$$\begin{aligned} \lambda \frac{\partial T}{\partial u} &= -e^{-k_T u} \int_{u_-}^u d\tilde{u} Q(\tilde{u}) e^{k_T \tilde{u}} \\ &= - \int_{u_-}^u d\tilde{u} Q(\tilde{u}) + k_T \int_{u_-}^u d\tilde{u} \int_{u_-}^{\tilde{u}} d\tilde{\tilde{u}} Q(\tilde{\tilde{u}}) + O(l_I^3 k_T^3). \end{aligned} \quad (45)$$

Here k_T is the thermal wave number of a curved interface,

$$k_T = \frac{V_n C}{\lambda} + 2K_0. \quad (46)$$

Expansion (45) is in increasing powers of k_T and may be considered an expansion into ‘‘powers of disequilibrium.’’ It can be truncated if $l_I k_T \ll 1$, which, in addition to condition (22), requires the generalized Peclet number to be small,

$$Pe \equiv l_I V_n C / \lambda \ll 1. \quad (47)$$

Then the temperature gradient in Eq. (45) can be calculated using the equilibrium structure of the OP $\eta_I(u)$ for the heat-source density in the energy representation,

$$Q(u) = V_n \frac{d\eta_I}{du} \left[\left(\frac{\partial e}{\partial \eta} \right)_{v,T} - \kappa_E \left(\frac{d^2 \eta_I}{du^2} + 2K_0 \frac{d\eta_I}{du} \right) \right]. \quad (48)$$

Finally, substitution of Eq. (45) into Eq. (44b) gives us the expression for the Gibbs–Duhem force,

$$F_{GD} = - \frac{V_n}{\lambda} \left(J_1 - \frac{C}{\lambda} V_n J_2 - 2K_0 J_3 \right). \quad (49)$$

The coefficients J_i 's are different moments of the entropy density and can be represented as follows:

$$\begin{aligned} J_1 &= \int_{u_-}^{u_+} du (\check{s} - s_+) U(u), \\ J_2 &= \int_{u_-}^{u_+} du (\check{s} - s_+) \int_{u_-}^u d\tilde{u} U(\tilde{u}), \\ J_3 &= \int_{u_-}^{u_+} du (\check{s} - s_+) \int_{u_-}^u d\tilde{u} \left\{ \kappa_E \left(\frac{d\eta}{d\tilde{u}} \right)^2 + U(\tilde{u}) \right\}, \end{aligned} \quad (50)$$

$$U(u) = \check{e} - e_- = T_E (\check{s} - s_-).$$

Substitution of Eq. (49) into Eq. (44a) yields the evolution equation for the interface motion,

$$\begin{aligned} L \frac{T_E - T_-}{T_E} + \frac{1}{2} C \frac{[T]^2}{T_-} &= \left(\frac{\sigma}{m} + \frac{J_1}{\lambda} \right) V_n + 2\sigma K_0 - \frac{C}{\lambda^2} J_2 V_n^2 \\ &\quad - \frac{2}{\lambda} J_3 V_n K_0. \end{aligned} \quad (51)$$

Equation (51) is a new result. According to Eq. (49), the GD force is either parallel or antiparallel to the interfacial velocity and manifests in the second term proportional to the interfacial velocity in the evolution Eq. (51). Notice that σ/m is positive even for $\kappa < 0$, see Eq. (10). Exact expressions for the quantities J_i 's for different types of interfaces will be found in the next sections. It is instructive, however, to elucidate the physical nature of the terms in Eq. (51) using only

measurable quantities such as the latent heat L and the relative surface entropy Γ_s , Eq. (12). From Eqs. (50) one can see that $J_3 \approx J_2 \approx J_1 l_I$. Then, if $\kappa_s = 0$, the entropic representation yields

$$\begin{aligned}
 J_1 &= T_E \int_{u_-}^{u_+} du \{s(u) - s_+\} \cdot \{s(u) - s_-\} \\
 &= T_E \int_{u_-}^{u_+} du \left\{ \delta s^2 + 2 \frac{[s]}{[\eta_I]} (\eta_I - \bar{\eta}) \delta s \right. \\
 &\quad \left. + [s]^2 \frac{(\eta_I - \eta_-)(\eta_I - \eta_+)}{[\eta_I]^2} \right\}, \tag{52}
 \end{aligned}$$

where $\bar{\eta} = (\eta_- + \eta_+)/2$. Using the bell-like shape of δs from Eq. (12), we obtain

$$\begin{aligned}
 \int_{u_-}^{u_+} du \delta s^2 &\approx \frac{1}{l_I} \Gamma_s^2, \quad \int_{u_-}^{u_+} du (\eta_I - \bar{\eta}) \delta s \approx 0, \\
 \int_{u_-}^{u_+} du \frac{(\eta_I - \eta_-)(\eta_I - \eta_+)}{[\eta_I]^2} &\approx -\frac{1}{6} l_I. \tag{53}
 \end{aligned}$$

Then, taking into account that $[s(T_E)] = L/T_E$, and substituting Eqs. (53) into Eq. (52), we obtain

$$J_1 \approx \frac{T_E}{l_I} \Gamma_s^2 - \frac{l_I}{6T_E} L^2. \tag{54}$$

The type of transition effects the relative magnitudes of Γ_s and L , which in turn dramatically effects the magnitude of J_1 , being negative for a typical first-order transition and positive for a continuous transition. Hence, see Eqs. (49), (54), F_{GD} propels the motion of interfaces that appear after first order transitions serving as a driving force and opposes motion of interfaces after continuous transitions manifesting a drag force. Substituting Eq. (54) into Eq. (51) we arrive at the linear approximation of the local evolution equation,

$$L \frac{T_E - T_-}{T_E} = 2\sigma K_0 + \left(\frac{\sigma}{m} - \frac{l_I}{6\lambda T_E} L^2 + \frac{T_E}{\lambda l_I} \Gamma_s^2 \right) V_n. \tag{55}$$

The beauty of this equation is that it is expressed only through measurable quantities and appropriate thermodynamic parameters of a system and still is applicable to many different situations.

D. Heat-balance equation

The heat equation (37) accounts for the thermal fluxes across and along the interface. Consequently there is no conservation of energy along the characteristic line $(v, w) = \text{const}$, while such conservation exists in the case of a planar interface where $K = 0$. Absence of the conservation law does not allow us to resolve the large-scale thermal problem for a curved interface, which has been done for a planar one in Ref. 41. To analyze the flow of energy through the interface we need to calculate the energy density flux vector in the interface. Equations (15), (36), (45), (48) yield

$$\begin{aligned}
 J_E &= -\lambda \frac{dT}{du} + \kappa_E V_n \left(\frac{d\eta_I}{du} \right)^2 \\
 &= V_n (\hat{e} - e_-) + O(\text{Pe}^2 + \text{Pe Ge}). \tag{56}
 \end{aligned}$$

The most important ramification of the energy density flux, Eq. (56), is the presence of temperature gradients in the interfacial transition region even when outside the interface isothermal conditions are maintained. To find the equation for the jumps of temperature and temperature-gradient across a curved interface we average the stationary GHE (37) ($\partial T/\partial t = 0$) in the interval (u_-, u_+) , use the same ideas as in Eq. (40) and obtain the heat balance equation,

$$\lambda \left(\left[\frac{\partial T}{\partial u} \right] + k_T [T] \right) + V_n (L - 2\epsilon K_0) = 0. \tag{57}$$

Equation (57) differs from the regular heat-balance (Stefan) boundary condition in the term proportional to the curvature of the interface K_0 and the velocity of its motion V_n . Another way to look at the condition (57) is to say that the heat of transformation is less than the latent heat times the transformed volume by the amount of the surface internal energy times the area of the new interface. The latter constitutes the *surface creation and dissipation effect*, which vanishes for a flat or immobile interface when the interfacial area does not vary. This effect is totally missing from the formulation in Refs. 8, 9 because $\kappa_E = 0$ is assumed there.

IV. HOMOPHASE INTERFACES

Homophase interfaces (HOI) appear after a continuous transition, when on both sides of the interface are different variants of the same phase. Antiphase domain boundaries, magnetic domain walls and cosmological walls are examples of HOI's. The motion of HOI has been addressed in numerous studies, which go back to Lifshitz's seminal paper,⁴² where he conjectured a linear proportionality between the speed and curvature of a moving antiphase domain boundary. Allen and Cahn²⁷ used a continuum approach, similar to that of the present paper, and, on the premise of the invariable interfacial profile of the moving isothermal HOI in the direction of its motion, showed that a small piece of a gently curved interface, condition (22), will move with the velocity, $V_n = -2mK_0$. Krzanowski and Allen,⁴³ and Cahn and Novick-Cohen³⁹ considered solute-drag effects at a migrating HOI. Umantsev¹³ considered the influence of the internal energy excess on the dynamics of HOI in the framework of the Onsager theory of linear response and showed that such excess causes drag effect on the motion of HOI. The drag alters the effective interfacial mobility as follows:

$$V_n = -\frac{m}{1 + D_0} \cdot 2K_0. \tag{58}$$

In the denotations of the present paper the drag coefficient is $D_0 = m\chi\epsilon/\lambda\sigma l_I$. Equation (58) shows that the interfacial dynamics is limited not only by the mobility of an interface but also by the thermal conduction with the drag coefficient D_0 measuring the relative role of these processes.

A number of questions, however, remained unaddressed by the simplified Onsager-type formulation in Ref. 13. For instance, what is the temperature distribution around the interface? What is the mechanism of thermal drag? What will happen if the energy transfer mechanism (thermal conduc-

tion) is turned off? In order to answer these questions we shall carry out here a continuum analysis of HOI motion.

A. Continuum theory

The free energy g for a system undergoing continuous transition must be an even function of OP because states with $\pm \eta$ are indistinguishable. This makes the coefficient b in Eq. (3) vanish. In the present study we choose a regular Landau form for the free energy,

$$g = g_\alpha(T) + \frac{1}{2} a_0 \eta^2 \left(\frac{T - T_c}{T_c} + \frac{1}{2} \eta^2 \right). \quad (59)$$

The homogeneous equilibrium set $\eta^E = \Xi(T_E)$ for such free energy, Fig. 2(a), consists of a totally disordered α -state with $\eta_\alpha = 0$ and two ordered variants of the same phase, β and γ , with $\eta_\beta = \pm \sqrt{-\tau}$, where

$$\tau = \frac{T_E - T_c}{T_c}. \quad (60)$$

Above the critical temperature T_C ($\tau > 0$) this set is reduced to only one completely disordered and stable α -state. Below T_C ($\tau < 0$) this set consist of homogeneous ordered phases η_β and η_γ with the disordered α -state being unstable. Stable heterogeneous isothermal solutions of Eq. (7), $\eta_i(x)$, exist at any $T_E < T_C$ ($\tau < 0$) and represent transition layers (HOI) where OP changes from η_γ to η_β over the distance $l_I = 2\sqrt{-2\kappa/a_0\tau}$. The surface energy of HOI is $\sigma = \frac{2}{3}\sqrt{-2\kappa a_0 \tau^3}$, Γ_s equals the surface entropy $\chi^\alpha(-\tau)^{1/2}$, and $\varepsilon \equiv T_E \chi$ because $\chi \gg \sigma/T_E$, see Eq. (23). Then, see Eqs. (49), (54), as $L=0$, $F_{GD} \sim -V_n$ (drag force) and Eq. (58) may be easily recovered from Eq. (55). Notice that in the framework of the continuum theory the drag coefficient D_0 does not show critical behavior near T_C , cf. Eq. (63) below. This is a consequence of a linear temperature dependence of the first term of the Landau expansion (59).

In order to derive the continuum evolution equation (51) for HOI one has to calculate the coefficients J_i 's from Eqs. (50) for the free energy (59),

$$J_1 = \frac{\sqrt{2}a_0}{3T_c} \sqrt{a_0\kappa(1+\tau)(-\tau)^{3/2}}, \quad (61)$$

$$J_2 = \frac{a_0\kappa}{T_c} (1+\tau)(-\tau), \quad J_3 = \frac{2a_0\kappa}{3T_c} \tau^2.$$

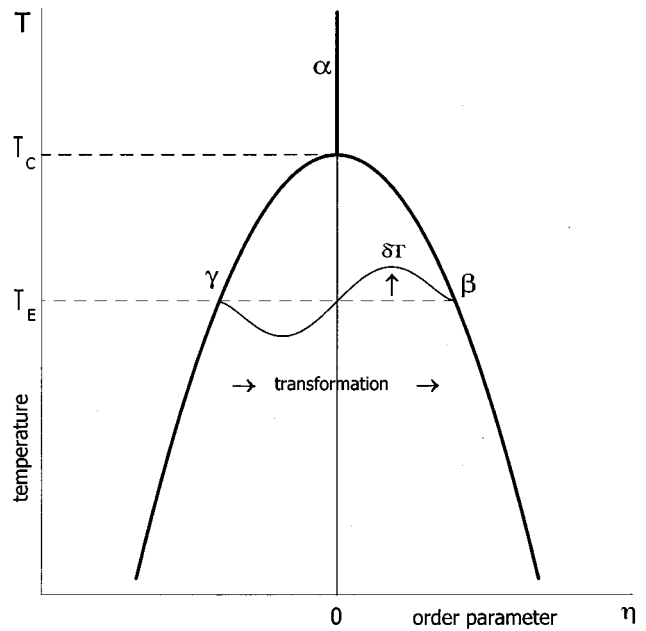
Substitution of Eqs. (61) into (51) yields the evolution equation for HOI motion in the form,

$$V_n + 2mK_0 + DV_n \left\{ 1 - \frac{3}{4} \left(\text{Pe} + \frac{1+\tau/3}{1+\tau} \text{Ge} \right) \right\} = 0, \quad (62)$$

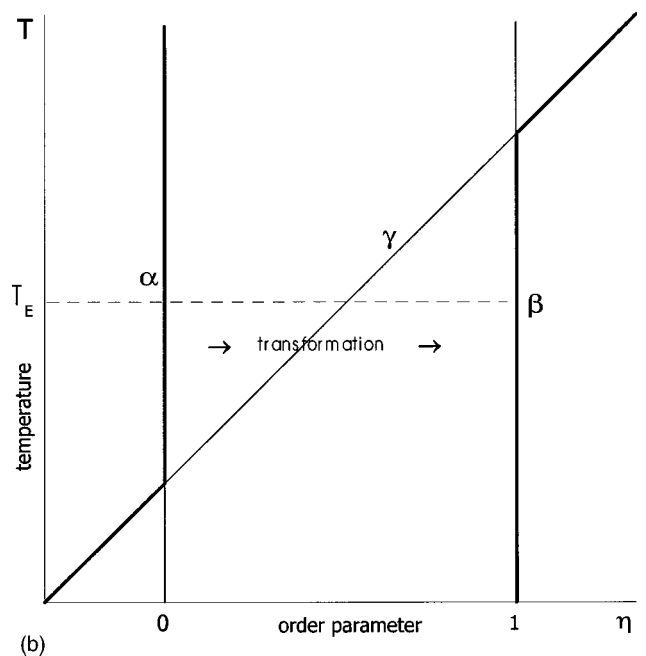
where the continuum-theory drag coefficient D is

$$D = \frac{1+\tau}{2\theta R}, \quad \theta = \frac{CT_c}{a_0}. \quad (63)$$

There are two corrections to the interface evolution equation (62) due to the temperature gradients in the transition region. The linear correction DV_n does not vanish even for slightly



(a)



(b)

FIG. 2. Homogeneous equilibrium states for different types of phase transitions. Thick lines stable states; thin solid lines, unstable states. (a) Continuous transition, curved thin line, the temperature double layer $\delta T(\eta)$; (b) first-order transition.

curved and thus slowly moving pieces of interface. The second-order dissipative correction $D(\text{Pe} + \text{Ge})V_n$ is small due to the constraints (22), (47).

To explain the drag effect we propose a borrow-return mechanism, see Fig. 3. Both variants on either side of the interface are characterized by the same amount of internal energy density. Transformation inside the interface from one variant to the other, however, requires crossing the internal energy barrier (maximum), which corresponds to the disordered phase with $\eta_\alpha = 0$. So, a small volume of substance

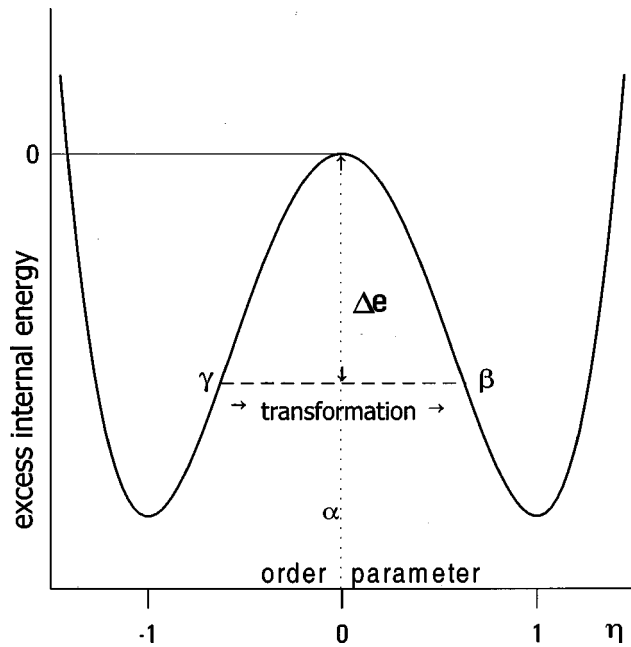


FIG. 3. Borrow-return mechanism. Internal energy of a substance as a function of an order parameter.

must borrow a certain amount of energy proportional to Δe from the neighboring volumes while moving uphill on the internal energy diagram, Fig. 3, and return it later on the downhill stage of the transformation. The borrow-return mechanism entails the internal energy flux vector, which can be calculated from Eqs. (56), (59),

$$J_E = \frac{1}{4} a_0 (\eta^4 - \eta^2 - \tau^2 - \tau) V_n. \quad (64)$$

This is a bell-like function of space, peaked at $u=0$ ($\eta = 0$). Such internal energy exchange requires a transport mechanism, which is served here by the heat conduction. Thus, the drag effect is due to the finite rate of such mechanism measured by the conductivity λ .

The energy flux through the interface is manifested in the temperature waves of amplitude $[T]$, which can be calculated using Eq. (57). Assuming that $[dT/du]=0$ and using Eq. (58) to estimate the velocity of HOI, we arrive at the expression for the amplitude of the temperature waves,

$$[T] = -\frac{2\epsilon K_0}{C(R-1+RD)} \approx -2T_E \chi \frac{m}{\lambda} K_0 \alpha (-\tau)^{1/2}. \quad (65)$$

Notice that the surface energy ϵ and entropy χ have the critical temperature dependence, which yields the critically dependent temperature jump.

B. Dissolution of a spherical particle

Different thermal effects of HOI motion may be elucidated in a problem of dissolution of a γ -phase (minority-variant) spherical particle in a β -phase (majority-variant) infinite matrix. Such a situation occurs after quenching material to temperatures below the critical point T_C . For a spherical particle $K_0 = 1/r_0$ and $V_n = dr_0/dt$, where $r_0(t)$ is the particle's radius. Then, Eq. (62) may be approximately solved as follows:

$$(1+D)(r_{in}^2 - r_0^2) - 2Dr^*(r_{in} - r_0) = 4mt, \quad (66)$$

where r_{in} is the initial radius of a particle and r^* is the threshold radius, below which the thermal effect changes from drag to boost,

$$r^* = \frac{3/2}{1+\tau} \left(1 + \frac{\tau}{3} - 2\theta \frac{D}{1+D} \right) l_I. \quad (67)$$

The threshold radius r^* , however, is of the order of the magnitude of the interfacial thickness and, obviously, the interface approximation, which was used all along to derive Eq. (62) is not valid for $r_0 < r^*$.

For the total dissolution time of a minority-variant spherical particle, Eq. (66) yields

$$\bar{t} = \frac{r_{in}^2}{4m} (1+D) \left(1 - 2 \frac{D}{1+D} \frac{r^*}{r_{in}} \right), \quad (68)$$

The first term in this expression represents the solution of this problem rendered by athermal LAC theory.^{27,42} The second term represents the thermal correction given by Onsager-type macroscopic theory.¹³ The third term is the continuum correction due to dissipative processes inside the interface considered in the present treatment.

To verify the evolution equation for HOI motion, Eq. (62), we shall use the method of numerical simulations to solve the above described problem of dissolution of a spherical particle. This method allows one to study the dynamics of interfacial motion without simplifying assumptions of scale separation, Eqs. (22), (47) and the averaging technique. The problem of dissolution was simulated by the coupled Eqs. (14), (33), (59) and the computations were conducted in the scaled units with the spatial l_η and temporal τ_η scales,

$$l_\eta = \sqrt{\frac{\kappa}{a_0}}, \quad \tau_\eta = \frac{1}{\gamma a_0}. \quad (69)$$

For a spherically symmetric problem all surfaces $U = \text{const}$ are concentric spheres with the radii of curvature $r = r(t)$. At $r \rightarrow +\infty$ the β -phase remained for the entire computational period, while at $r = 0$ γ -phase existed up until the last stages of dissolution, Fig. 1. For dissolution $V_n < 0$ with different dynamical regimes being controlled by the average temperature τ , Eq. (60), thermodynamic ratio θ , Eq. (63), and kinetic ratio R , Eq. (34). In Fig. 4 are shown the results of numerical solutions of Eqs. (14), (33), (59) for different values of r_{in} in the form of the normalized total dissolution times ($4m\bar{t}/r_{in}^2$) vs the drag coefficient D (values of θ , τ were kept constant while R changed). If LAC theory were correct the numerical values of the function ($4m\bar{t}/r_{in}^2$) would have been equal to unity. In fact, the normalized total dissolution times deviate from unity significantly and are very close to $(1+D)$, a correction required by the macroscopic Onsager-type theory of thermal effects, Eq. (58). The numerical results, however, are smaller than the Onsager correction, in accordance with the formula (68), which takes into account dissipative effects inside the interface. The proximity of the numerical dissolution times to the continuum-theory values for different r_{in} and D [see Eq. (68) and thin lines in Fig. 4] proves the validity of the local dynamic Eq. (62).

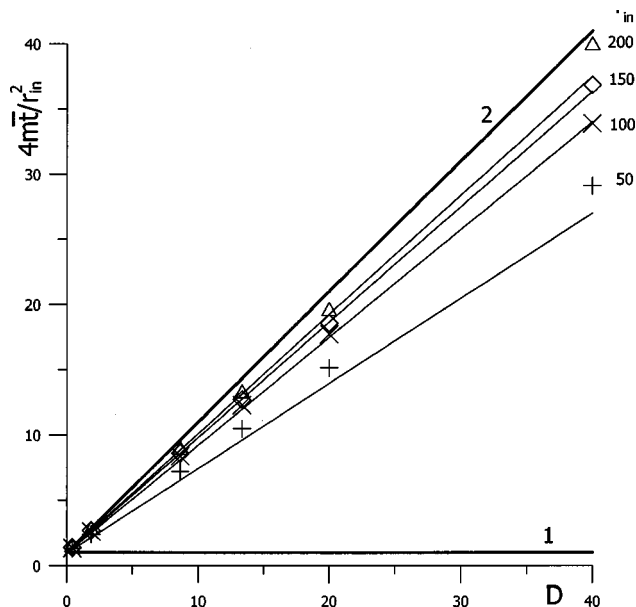


FIG. 4. Scaled total dissolution times vs the drag coefficient D for different initial radii of spherical particles: $r_{in}=200$ (Δ); $r_{in}=150$ (\diamond); $r_{in}=100$ (\times); $r_{in}=50$ ($+$). Solid lines, theoretical results: 1, athermal LAC theory; 2, thermal macroscopic Onsager-type theory; thin lines, continuum theory, Eq. (68), for different initial radii.

As it has been explained in the previous subsection, the energy flux manifests in the temperature waves of amplitude $[T]$, Eq. (65). To verify this prediction we have examined in the numerical experiment the critical dependence of $[T]$ on the average temperature of the medium τ . The crosses in Fig. 5 correspond to the numerical values of $[T]/T_C$, the solid line is the best-fit function $[T]/T_C = 5.4 \times 10^{-3} \times (-\tau)^{1/2}$. While the numerical critical exponent is very close to the theoretically predicted exponent of $\frac{1}{2}$, the numerical prefactor differs by 50% from the theoretical value of 7.9×10^{-3} for

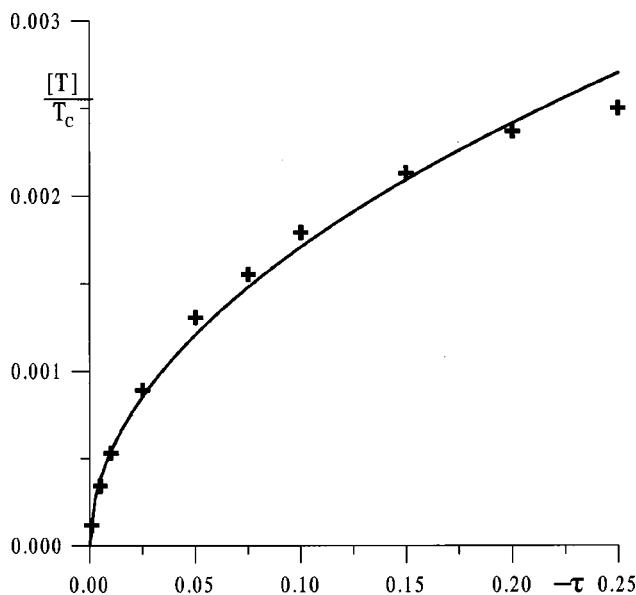


FIG. 5. Amplitude of the temperature wave $[T]/T_C$ as a function of the distance from the critical point $(-\tau)$ for $r_{in}=200$, $\theta=0.15$, $R=10$.

this experiment. The reason for such discrepancy is the assumption $[dT/du]=0$, which is not completely true.

C. Ideal thermal insulator

According to Eqs. (58), (62) HOI slows down and stops completely if $\lambda \rightarrow 0$, implying that the simultaneous Eqs. (14), (33), (59) have an equilibrium non-one-dimensional solution for an ideal thermal insulator that is, a substance with $\lambda=0$, if such a substance would exist. Rigorously speaking Eqs. (58) and (62) are not valid for vanishing λ because small thermal conductivity represents a singular perturbation to the problem, e.g., condition (47) is not fulfilled. Physically this means that phase transition and temperature variation occur on the same length scale and the separation of the thermal and interfacial length scales is not possible. To analyze theoretically the HOI structure in an ideal insulator one has to solve directly the equilibrium Eq. (6), which is known not to have stable isothermal inhomogeneous solutions others than 1D. However, if the condition of invariable temperature is relaxed, there appears a solution, which, to the second order in Ge , takes the form,

$$\delta T \equiv \frac{T(u) - T_E}{T_C} \approx -\sqrt{2} l_\eta K_0 \frac{\eta_I}{\tau^2} (8\tau + 7\eta_I^2)(\tau + \eta_I^2), \quad (70)$$

$$\delta \eta \equiv \eta(u) - \eta_I(u) \approx -\sqrt{2} l_\eta K_0 \frac{\eta_I^2}{\tau^2} (\tau + \eta_I^2).$$

This solution represents a *temperature double layer* δT in the transition zone that causes small OP spikes $\delta \eta$.

Vanishing of the velocity of motion of a curved HOI in an ideal insulator is a striking result. Physically this means that a network of HOI's will be *at equilibrium* with an ideal insulator. Thus it becomes crucial to check the stability of these states with respect to dynamic fluctuations. Analytical evaluation of stability is somewhat tedious task. The method of numerical simulations has an advantage of finding only stable solutions, as "fluctuations" are naturally present there in the form of computational errors. In Fig. 6 are depicted spatial distributions of the temperature increments δT for a spherical particle with initial radius $r_{in}=100$ in a system with $\theta=0.1$ and average temperature $\tau=-0.1$, obtained numerically for $R=1$ and $R=0$. In Fig. 7 the increments of temperature δT (a) and OP $\delta \eta$ (b) are plotted as functions of the OP η after a very long computational time in a system with $R=0$. The temperature double layer δT as a function of the OP η is also shown in Fig. 2(a), although greatly exaggerated. Comparison of the simulation results with the theoretical expressions (70) in Fig. 7 provides a good match, which convincingly demonstrates the *existence and stability* of a network of HOI's with the temperature double layer. In a poorly conducting material this network will coarsen, the coarsening process, however, will be totally controlled by the heat transfer.

V. HETEROPHASE INTERFACES

Heterophase interfaces (HTI) separate contiguous phases of the same medium, but different symmetries and appear as a result of a first order (discontinuous) transition. The coef-

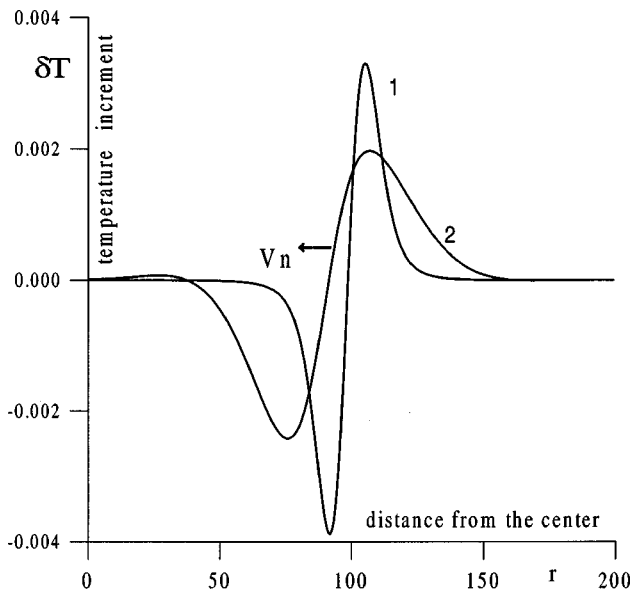


FIG. 6. The temperature double layers δT as a function of the distance from the center of a spherical particle with $r_{in} = 100$ in a system with $\theta = 0.1$ and $\tau = -0.1$. Curve 1, $R = 0$; curve 2, $R = 1$. Arrow points in the direction of motion of layer 2.

coefficients of the Landau free energy may be chosen as follows: $a(T) = a_0(T - T_c)$, and b, c as temperature independent. Isothermal interface-dynamics effects in a system described by such free energy have been thoroughly investigated.²⁶ With all the due respect to these works, unfortunately, we should say that such free energy is too complicated for the purposes of analytical study of thermal effects, with the main difficulty coming from the temperature dependent latent heat of such system. In one of the earlier papers⁴¹ we have developed a more convenient model represented by the following free energy:

$$g = g_\alpha(T, P) + \frac{1}{2} a_0 \eta^2 \left\{ h - \frac{2}{3} (h + 2) \eta + \eta^2 \right\},$$

$$h = \frac{T - T_c}{T_E - T_c}. \quad (71)$$

High and low symmetry phases correspond to $\eta_\alpha = 0$ and $\eta_\beta = 1$ respective values of OP at all temperatures. These phases are separated by an equilibrium state with the temperature dependent value of OP $\eta_\gamma = \frac{1}{2} h(T)$, which is unstable above T_c , but gains thermodynamic stability below T_c , Fig. 2(b). A first order transition from α to β phase is accompanied by the release of the latent heat L in the same amount at all temperatures. In accordance with the Gibbs phase rule, the thermodynamic equilibrium between β and α phases, see Eq. (8), is achieved at the specific temperature $T_E = T_c / (1 - a_0/6L)$ only. For the free energy, Eq. (71), the relative surface entropy vanishes $\Gamma_s = 0$; the thickness $l_l = 4l_\eta$ and the surface energy $\sigma = \frac{1}{6} \sqrt{\kappa a_0}$ are temperature independent and, hence, remain unchanged even away from equilibrium. The coefficients J_i of the Gibbs–Duhem force, Eq. (50), are

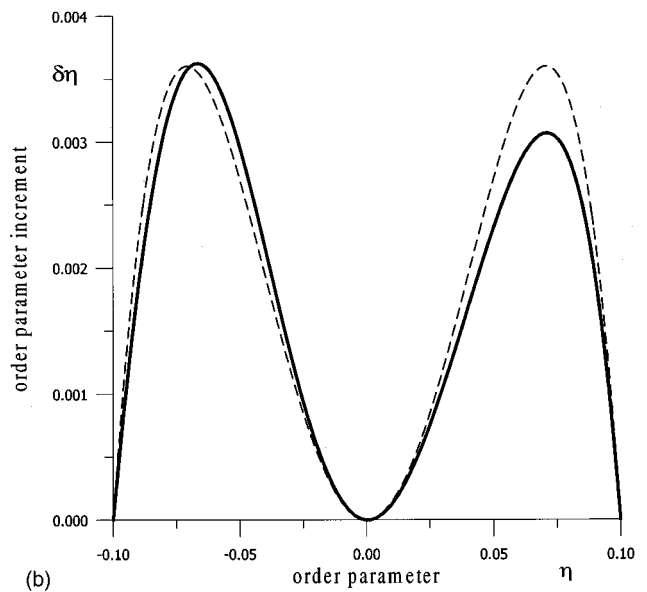
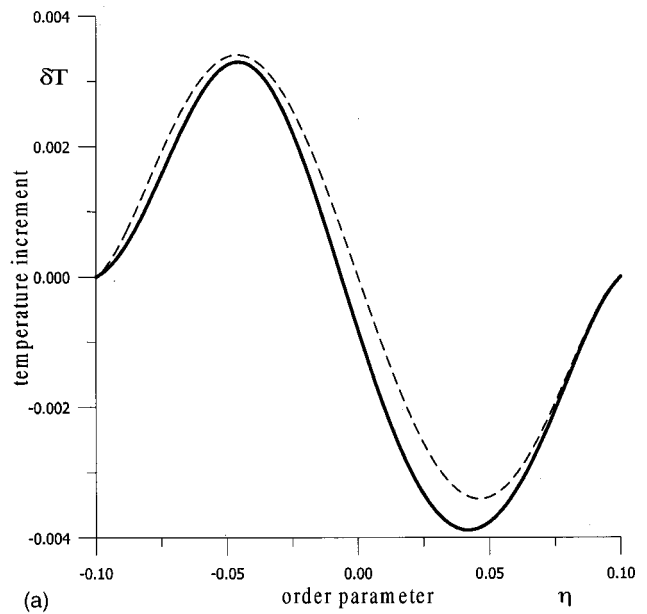


FIG. 7. Increments of temperature δT (a) and order parameter $\delta \eta$ (b) for $r_{in} = 100$ in a system with $\theta = 0.1$, $\tau = -0.1$, and $R = 0$ as functions of the order parameter η , compared with the analytical expressions (70) (dashed lines).

$$J_1 = -0.633 l \frac{L^2}{\eta T_E}, \quad J_2 = -0.645 l^2 \frac{L^2}{\eta T_E},$$

$$J_3 = -0.645 l^2 \frac{L^2}{\eta T_E} + 0.106 l^2 \frac{aL}{\eta T_E}. \quad (72)$$

A. Heat trapping

To reveal different thermal effects during first order transitions we shall consider a typical problem of growth of a spherical particle of the β -phase from the α -phase matrix. The r -axis is directed from β -phase to α -phase, Fig. 1, so that the center of curvature is in the β -phase and the growth of the particle corresponds to V_n being positive. Thermal effects do not change significantly the critical nucleus radius,

$r_{cr} \approx 2\sigma T_E / L(T_E - T_-)$, unless $\lambda \rightarrow 0$, see Eqs. (51) and (55). The rate of transformation, however, is different from the isothermal value. The most dramatic thermal effect, as can be seen from Eqs. (51) and (55), is manifested in the possibility to have β -phase growing ($V_n > 0$) even when its temperature after transformation is above the equilibrium value ($T_- > T_E$). This effect has been called *heat trapping* and was studied in detail in Refs. 11, 3, 4, 41. The heat trapping becomes possible when the Gibbs–Duhem force, Eq. (49), becomes large enough to propel an interface against the negative bulk driving force. As one can see from Eq. (55), for the heat trapping to occur the coefficient in front of the term linear in V_n must be negative and, as $\Gamma_s = 0$, the following criterion must be fulfilled:

$$\frac{l_l L^2}{\sigma T_E} > 6 \frac{\lambda}{m}. \quad (73)$$

Criterion (73) should be considered as the low limit on the thickness of the interface or the upper limit on the rate of thermal conduction in the system for the heat trapping to occur. During heat trapping the low symmetry β -phase grows at the expense of the high symmetry α -phase at a temperature above the equilibrium point. In case of crystallization of water this would have meant the growth of superheated ice from supercooled water. Condition (73), however, is not fulfilled for crystallization of ice but is quite feasible for crystallization of other substances.

Equations (51) and (55) also point at another situation when the growing phase may be observed at a temperature above equilibrium one that is, around regions in materials where the curvature is negative (the center of curvature is in the α -phase). The difference with the heat trapping effect is that the latter is possible even for flat interfaces.

B. Surface creation and dissipation effect

Another example of a thermal effect can be revealed in the analysis of the heat balance before and after a HTI sweeps material during a first order transition. The amount of heat released is called the heat of transformation. It is commonly attributed to the product of the latent heat and the transformed volume. However, as Eq. (57) demonstrates, if the moving interface is curved, the heat of transformation will differ from the above described amount by the amount of the surface internal energy times the surface area created or destroyed. This effect has been noticed by Wollkind in Ref. 44 and used in the form of a boundary condition in one of his later papers. Tiller discussed the surface creation or destruction effect in Ref. 45. The theoretical description of this effect in Ref. 45, however, was not appropriate because the author attributed it to the evolution equation, similar to Eq. (55), instead of the heat-balance condition, Eq. (57).

The rigorous derivation of the surface creation and dissipation effect has been given by Roytburd and the present author in Ref. 11, and used by Davis and the present author in Ref. 46 to study the influence of this effect on the absolute stability of the solidification front during crystal growth from a hypercooled melt, i.e., the condition when the front loses dendritic or cellular structure and restores completely its

smoothness. If the surface creation and dissipation effect is not considered the absolute stability is achieved when the thermal length $l_T = \alpha / V_n$ becomes equal to the capillary length $l_C = \sigma C T_E / L^2$.⁴⁷ A consistent account of the surface creation and dissipation effect shows that stabilization occurs when l_T becomes equal to $l_C(1 - L/CT_E)$, that is, for larger front speeds and initial hypercoolings. This means that the surface creation and dissipation effect works “against” the regular Gibbs–Thompson effect and retards stabilization.

VI. DISCUSSION

In summary, we have presented theoretical description of a few thermal effects in interface motion. These effects are robust and conceivably independent of the method employed for the analysis. Equations (51) and (57) identify the local interfacial variables V_n , K_0 , T_- , $[T]$, $[dT/du]$, and relate them to the kinetic properties of the medium like α , m and thermodynamic interface quantities, L , σ , ε , Γ_s , l_l . These equations are local in the sense that they are independent of the history of the process and may be used as boundary conditions in a global problem of structural evolution like that of dendritic growth in crystallization or domain growth after continuous ordering.

There are two distinctly different sets of thermal effects considered in this paper. One set originates from the existence of the Gibbs–Duhem thermodynamic force on the interface, which is one of the principal results of the present paper. In the cases of continuous and discontinuous transitions this force has opposite directions compared to the velocity of the interface, resulting in heat trapping effect for the latter transition and drag effect for the former one. Interestingly to note that thermal drag during continuous transitions exists despite of the vanishing latent heat, which causes thermal effects during first order transitions, e.g., crystallization. Thermal drag occurs because the conversion of one variant of the same phase into another one is accompanied by the transmission of energy between neighboring pieces of a material, which cannot occur infinitely fast. The Gibbs–Duhem force is antiparallel to the boundary velocity and has the meaning of a drag force. As a result, HOI moves towards the center of its curvature with a speed which is lower than that predicted by the Lifshitz–Allen–Cahn theory.^{27,42} Such slowing down should be taken into account in experimental verification of the theory of coarsening of domain structures albeit thermal effects do not change time exponents of the latter.

The present treatment convincingly demonstrated that the thermal conductivity of a material is vital for the structural coarsening. If the thermal conductivity vanishes ($\lambda = 0$), that is the energy-transfer mechanism is “turned off,” a curved homophase interface becomes stable. Stability of a minority-variant spherical particle in the bulk of a majority variant is quite surprising and needs a physical explanation inasmuch as a critical nucleus in the theory of the first order transitions is an equilibrium but *unstable* state of the system. “Dissolution” of a minority-variant spherical particle is caused by Laplacian pressure from the curved interface [Gibbs–Thompson effect, see Eq. (55)]. At the same time the

Gibbs–Duhem force generates an additional (thermal) pressure in the particle that neutralizes Laplacian pressure.

Another set of thermal effects stems from the existence of the surface internal energy and necessity to carry it over together with the moving interface. In the case of a discontinuous transition this entails the surface creation and dissipation effect, which consists in altering the heat of transformation by the amount of the internal energy of the surface area created or destroyed by the moving curved interface. In the case of a continuous transition the surface internal energy entails thermal waves around a moving interface. Temperature waves must accompany motion of antiphase-domain or grain boundaries and can be revealed by different imaging techniques and serve as experimental verification of the thermal drag effect. One possibility is *in situ* observation in infrared light. Another possibility is the Mirage technique measurement, which utilizes the gradients in the index of refraction of air arising from the temperature gradients induced by the temperature waves on the specimen surface.⁴⁸

ACKNOWLEDGMENT

This research was supported by the National Science Foundation through Grant No. DMR-0080176 from the Material Theory program.

- ¹N. S. Fastov, Zh. Eksp. Teor. Fiz. **22**, 487 (1952).
- ²A. Z. Patashinsky and I. S. Yakub, Zh. Eksp. Teor. Fiz. **73**, 1954 (1977) [Sov. Phys. JETP **46**, 1025 (1977)].
- ³A. Z. Patashinsky and M. V. Chertkov, Fiz. Tverd. Tela (Leningrad) **32**, 509 (1990) [Sov. Phys. Solid State **32**, 295 (1990)].
- ⁴S. A. Schofield and D. W. Oxtoby, J. Chem. Phys. **94**, 2176 (1991).
- ⁵B. I. Halperin, P. C. Hohenberg, and S.-K. Ma, Phys. Rev. B **10**, 139 (1974).
- ⁶G. Caginalp, Arch. Ration. Mech. Anal. **92**, 207 (1986); J. B. Collins and H. Levine, Phys. Rev. B **31**, 6119 (1985).
- ⁷G. Caginalp and W. Xie, Phys. Rev. E **48**, 1897 (1993); M. Plap and A. Karma, Phys. Rev. Lett. **84**, 1740 (2000).
- ⁸O. Penrose and P. Fife, Physica D **43**, 44 (1990).
- ⁹S.-L. Wang *et al.*, Physica D **68**, 189 (1993); S.-L. Wang and R. F. Sekerka, Phys. Rev. E **53**, 3760 (1996).
- ¹⁰L. D. Landau and E. M. Lifshitz, *Fluid Mechanics* (Pergamon, Reading, 1968), p. 183.
- ¹¹A. R. Umantsev and A. L. Roytburd, Sov. Phys. Solid State **30**, 651 (1988).
- ¹²R. K. P. Zia *et al.*, Mod. Phys. Lett. B **2**, 961 (1988).
- ¹³A. Umantsev, Acta Mater. **46**, 4935 (1998).
- ¹⁴F. P. Ludwig, J. Schmelzer, and A. Milchev, Phase Transitions **48**, 237 (1994).
- ¹⁵L. D. Landau, Phys. Z. Sowjetunion **11**, 26545 (1937); in *Collected Papers of L. D. Landau*, edited by D. Ter-Haar (Gordon and Breach, London, 1967), pp. 193, 209.
- ¹⁶L. D. Landau, Phys. Z. Sowjetunion **12**, 123 (1937); see also, *Collected Papers of L. D. Landau*, edited by D. Ter-Haar (Gordon and Breach, London, 1967), p. 236; V. L. Ginzburg and L. D. Landau, Zh. Eksp. Teor. Fiz. **20**, 1064 (1950).
- ¹⁷J. W. Cahn and J. E. Hilliard, J. Chem. Phys. **28**, 258 (1958).
- ¹⁸A. G. Khachatryan and R. A. Suris, Sov. Phys. Crystallogr. **13**, 63 (1968); W. I. Khan, J. Phys. C **19**, 2969 (1986); A. M. Grundland, E. Infeld, G. Rowlands, and P. Winternitz, J. Phys.: Condens. Matter **2**, 7143 (1990).
- ¹⁹P. Winternitz, A. M. Grundland, and J. A. Tuszynski, J. Phys. C **21**, 4931 (1988); A. E. Filippov, Yu. E. Kuzovlev, and T. K. Soboleva, Phys. Lett. A **165**, 159 (1992).
- ²⁰J. W. Gibbs, *The Scientific Papers* (Dover, New York, 1961), Vol. 1, p. 219.
- ²¹L. D. Landau and E. M. Lifshitz, *Statistical Physics* (Pergamon, Oxford, 1969), p. 455.
- ²²A. Umantsev, Phys. Rev. B **64**, 075419 (2001).
- ²³L. I. Mandel'shtam and M. A. Leontovich, Zh. Eksp. Teor. Fiz. **7**, 438 (1937) (in Russian).
- ²⁴L. D. Landau and E. M. Lifshitz, *Fluid Mechanics* (Pergamon, Reading, 1968), p. 305.
- ²⁵L. D. Landau and I. M. Khalatniko, Dokl. Akad. Nauk SSSR **96**, 469 (1954).
- ²⁶H. Metiu, K. Kitahara, and J. Ross, J. Chem. Phys. **65**, 393 (1976); Sai-Kit Chan, *ibid.* **67**, 5755 (1977).
- ²⁷S. M. Allen and J. W. Cahn, Acta Metall. **27**, 1085 (1979).
- ²⁸J. D. Gunton and M. Droz, *Introduction to the Theory of Metastable and Unstable States* (Springer-Verlag, New York, 1983), Vol. 183, p. 62.
- ²⁹S. A. Safran, *Statistical Thermodynamics of Surfaces, Interfaces, and Membranes* (Addison–Wesley, Reading, 1994), p. 80.
- ³⁰G. F. Mazenko, Phys. Rev. Lett. **63**, 1605 (1989).
- ³¹M. Born and E. Wolf, *Principles of Optics: Electromagnetic Theory of Propagation, Interference and Diffraction of Light*, 7th ed. (Cambridge University Press, New York, 1999).
- ³²H. Goldstein, *Classical Mechanics* (Addison–Wesley, Canada, 1980), p. 489.
- ³³C. Weatherburn, *Differential Geometry of Three Dimensions* (Cambridge University Press, Cambridge, 1927), p. 225.
- ³⁴R. Curant and D. Hilbert, *Methods of Mathematical Physics* (Interscience, New York, 1962), Vol. 2, p. 305.
- ³⁵E. A. Guggenheim, *Thermodynamics* (North–Holland, Elsevier, Amsterdam, 1967), p. 45.
- ³⁶I. M. Gelfand and S. V. Fomin, *Calculus of Variations* (Prentice–Hall, New York, 1963).
- ³⁷K. Binder, H. L. Frisch, and J. Jackle, J. Chem. Phys. **85**, 1505 (1986); H. G. Rotstein *et al.* (Preprint, Technion, Israel).
- ³⁸M. E. Gurtin and A. C. Pipkin, Arch. Ration. Mech. Anal. **31**, 113 (1968); J. W. Nunziato, Q. Appl. Math. **24**, 187 (1971); H. G. Rotstein, A. Nepomnyashchy, and A. Novick-Cohen, J. Cryst. Growth **198/199**, 1262 (1999).
- ³⁹J. W. Cahn and A. Novick-Cohen, Acta Mater. **48**, 3425 (2000).
- ⁴⁰E. A. Guggenheim, *Thermodynamics* (North–Holland, Elsevier, Amsterdam, 1967), p. 121.
- ⁴¹A. Umantsev, J. Chem. Phys. **96**, 605 (1992).
- ⁴²I. M. Lifshitz, Sov. Phys. JETP **15**, 939 (1962).
- ⁴³J. E. Krzanowski and S. M. Allen, Acta Metall. **34**, 1035 (1986).
- ⁴⁴D. J. Wolkind, in *Preparation and Properties of Solid State Materials*, edited by W. R. Wilcox (Dekker, New York, 1979), Vol. 4, p. 111.
- ⁴⁵W. A. Tiller, *The Science of Crystallization: Microscopic Interfacial Phenomena* (Cambridge University Press, Cambridge, 1991), pp. 68, 99.
- ⁴⁶A. Umantsev and S. H. Davis, Phys. Rev. A **45**, 7195 (1992).
- ⁴⁷M. L. Frankel, Physica D **27**, 260 (1987).
- ⁴⁸E. J. Gonzalez, D. Josell, J. E. Bonevich, G. R. Stafford, and G. White (NIST, preprint, 1999).